

# Quark Stars and Color Superconductivity: A GRB connection ?

*Rachid Ouyed*  
*Nordic Institute for Theoretical Physics (NORDITA)*  
*Blegdamsvej 17*  
*DK-2100 Copenhagen Ø, Denmark*

## Abstract

At this conference many interesting talks were presented on the plausible existence of Quark Stars. Other talks dealt with the exotic new phases of quark matter at very high density. Here, I show how combining these two elements might offer a new way of tackling the Gamma Ray Burst puzzle.

## 1 Introduction

It is widely accepted that the most conventional interpretation of the observed Gamma-ray bursts (GRBs) result from the conversion of the kinetic energy of ultra-relativistic particles to radiation in an optically thin region [1, 2, 3, 4]. The particles being accelerated by a fireball mechanism (or explosion of radiation) taking place near an unknown central engine [5, 6, 7]. The first challenge is to conceive of circumstances that would create a sufficiently energetic fireball. In the model presented in this talk, the approach is to make use of intrinsic properties of quark stars (where exotic phases of quark matter come into play) to account for the fireball.

Quark matter at very high density is expected to behave as a color superconductor (see Figure 1). A novel feature of such a phase (in the 2-flavor case; hereafter 2SC) is the generation of glueball like particles (hadrons made of gluons) which as demonstrated in [8] immediately decay into photons. If 2SC sets in at the surface of a quark star the glueball decay becomes a natural mechanism for a fireball generation; a mechanism which is fundamentally different from models where the fireball is generated via a collapse [9, 10, 11] or conversion (of neutron star to quark star [12, 13, 14]) processes. I will then show how and why quark stars might constitute new candidates for GRB inner engines [15].

## 2 Quark stars and the 2SC phase

We first assume that quark stars exists in nature (further discussed in §7.2; see also Heiselberg and Bombaci in this volume) and constitutes the first major assumption in our model.

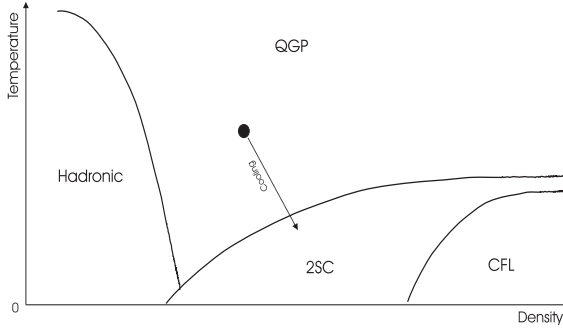


Figure 1: A schematic representation of a possible QCD phase diagram (see Alford in this volume). The arrow depicts a plausible cooling path of a quark star leading to the onset of color superconductivity in its surface.

## 2.1 Hot Quark stars

We are concerned with quark stars born with temperatures above  $T_c$  (the critical temperature above which thermal fluctuations will wash out the superconductive state). We shall refer to these stars as “hot” quark stars (HQSs) in order to avoid any confusion with strange stars which are conjectured to exist even at zero pressure if strange matter is the absolute ground state of strong interacting matter rather than iron [16, 17, 18, 19, 20].

Among the features of HQSs relevant to our model [19, 21, 22, 23]:

i) The “surface” of a HQS is very different from the surface of a neutron star, or any other type of stars. Because it is bound by the strong force, the density at the surface changes abruptly from zero to  $\rho_{HQS}$ . The abrupt change (the thickness of the quark surface) occurs within about 1 fm, which is a typical strong interaction length scale.

ii) The electrons being bound to the quark matter by the electro-magnetic interaction and not by the strong force, are able to move freely across the quark surface extending up to  $\sim 10^3$  fm above the surface of the star. Associated with this electron layer is a strong electric field ( $5 \times 10^{17}$  V/cm)- higher than the critical value ( $1.3 \times 10^{16}$  V/cm) to make the vacuum region unstable to spontaneously create ( $e^+, e^-$ ) pairs.

iii) The presence of normal matter (a crust made of ions) at the surface of the quark star is subject to the enormous electric dipole. The strong positive Coulomb barrier prevents atomic nuclei bound in the nuclear crust from coming into direct contact with the quark core. The crust [24] is suspended above the vacuum region.

iv) One can show that the maximum mass of the crust cannot exceed  $M_{crust} \simeq 5 \times 10^{-5} M_{\odot}$  set by the requirement that if the density in the inner crust is above the neutron drip density ( $\rho_{drip} \simeq 4.3 \times 10^{11}$  g/cc), free neutrons will gravitate to the surface of the HQS and be converted to quark matter. This is due to the fact that neutrons can easily penetrate the Coulomb barrier and are readily absorbed.

## 2.2 2SC and Light GlueBalls (LGBs)

The 2SC phase is characterized by five out of the eight gluons acquiring mass. The 3 massless gluons bind into LGBs. In [8] we studied properties of these LGBs. Those relevant to our present study are :

- i) The LGBs decay into photons with an associated lifetime of the order of  $10^{-14}$  s.
- ii) The mass of the LGBs is of the order of 1 MeV.

## 2.3 Cooling and 2SC layer formation

The HQS surface layer might enter the 2SC phase as illustrated in Figure 1. In the QCD phase diagram (Figure 2),  $(\rho_{\mathbf{B}_0}, T_{\mathbf{B}_0})$  is the critical point beyond which one re-enters the Quark-Gluon-Plasma (QGP) phase - illustrating the extent of the 2SC layer into the star. The star consists of a QGP phase surrounded by a 2SC layer where the photons (from the LGB/photon decay) leaking from the surface of the star provides the dominant cooling source. This picture, as illustrated in Figure 2, is only valid if neutrino cooling in the 2SC phase is heavily suppressed as to become slower than the photon cooling. Unfortunately, the details of neutrino cooling in the 2SC phase is still a topic of debate and studies ([25, 26] to cite only few). One can only assume such a scenario which constitutes the second major assumption in our model. In §6.2, we discuss the remaining alternative when photon cooling is dwarfed by neutrino cooling.

## 2.4 LGB decay and photon thermalization

The photons from LGB decay are generated at energy  $E_{\gamma} < T_c$  and find themselves immersed in a degenerate quark gas. They quickly gain energy via the inverse Compton process and become thermalized to  $T_c$ . We estimate the photon mean free path to be smaller than few hundred Fermi [27, 28] while the 2SC layer is measured in meters (see §4.2). A local thermodynamic equilibrium is thus reached with the photon luminosity given by that of a black body radiation,

$$L_{\gamma} = 3.23 \times 10^{52} \text{ ergs s}^{-1} \left( \frac{R_{HQS}}{5 \text{ km}} \right)^2 \left( \frac{T_c}{10 \text{ MeV}} \right)^4 . \quad (1)$$

The energy for a single 2SC/LGBs event is thus

$$\Delta E_{LGB} = \delta_{LGB} M_{2SC} c^2, \quad (2)$$

where  $M_{2SC} = \delta_{2SC} M_{HQS}$  is the portion of the star in 2SC. Here,  $\delta_{2SC}$  depends on the star's mass while  $\delta_{LGB}$  represent the portion of the 2SC that is in LGBs (intrinsic property of 2SC; see [8]). The photon emission/cooling time is then

$$\Delta t_{cool} = \frac{\epsilon M_{HQS} c^2}{L_\gamma}, \quad (3)$$

with  $\epsilon = \delta_{2SC} \delta_{LGB}$ .

## 3 Powering Gamma-Ray Bursts

### 3.1 Fireball and baryon loading

The fireball stems from the LGB decay and photon thermalization. The photons are emitted from the star's surface into the vacuum region beneath the inner crust ( $\sim 10^3$  fm in size). Photon-photon interaction occurs in a much longer time than the vacuum region crossing time. Also, the cross-section for the creation of pairs through interactions with the electrons in the vacuum region is negligible ([27, 28]). The fireball energy is thus directly deposited in the crust. If its energy density,  $aT_c^4$  (with  $a$  being the radiation density constant), exceeds that of the gravitational energy density in the crust, energy outflow in the form of ions occurs. More specifically, it is the energy transfer from photons to electrons which drag the positively charged nuclei in the process. One can show that the condition

$$aT_c^4 > \frac{GM_{HQS}}{R_{HQS}} \rho_{crust}, \quad (4)$$

where  $\rho_{crust}$  is the crust density and  $G$  the gravitational constant, is equivalent to

$$\left(\frac{T_c}{30 \text{ MeV}}\right)^4 > \left(\frac{M_{HQS}}{M_\odot}\right) \left(\frac{5 \text{ km}}{R_{HQS}}\right) \left(\frac{\rho_{crust}}{\rho_{drip}}\right), \quad (5)$$

which is always true if  $T_c > 30$  MeV. The fireball is thus loaded with nuclei present in the crust. Note that the 2SC layer is not carried away during the two-photon decay process because of the star's high gravitational energy density:  $\rho_{HQS}/\rho_{drip} \gg 1$ .

### 3.2 Episodic behavior

The star's surface pressure is reduced following photon emission<sup>1</sup>. A heat and mass flux is thus triggered from the QGP phase to the 2SC layer re-heating

---

<sup>1</sup>The pressure gradient in the 2SC layer is  $\Delta p \propto (8 - 5)T_c^4$  ([21]) where the massless gluons (3 out of 8) have been consumed by the LGB/photon process.

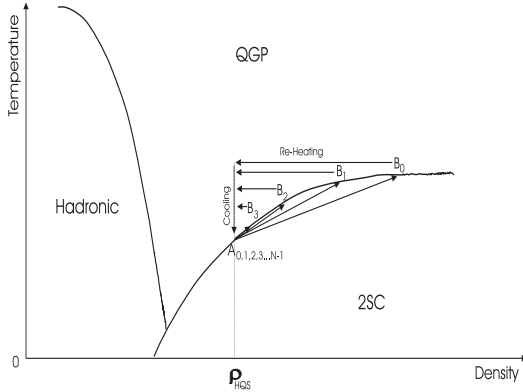


Figure 2: The episodic emission as illustrated in the QCD phase diagram. The 2SC front spreads deep inside the star and stops at  $\mathbf{B}_0$  before re-entering the QGP phase. Following photon cooling, heat flows from the core and re-heats the surface. The star then starts cooling until  $\mathbf{A}_1$  is reached at which point the stage is set for the 2SC/LGB/photon process to start all over again ( $\mathbf{A}_1 \rightarrow \mathbf{B}_1$ ) resulting in another emission.

(above  $T_c$ ) and destroying the superconductive phase. The entire star is now in a QGP phase (5 gluons  $\rightarrow$  8 gluons at the surface) and hence the cooling process can start again. This corresponds to the transition  $[\rho(\mathbf{B}_0), T(\mathbf{B}_0)] \rightarrow [\rho_{HQS}, T(\mathbf{B}_0)]$  in the QCD phase diagram (thermal adjustment). The stage is now set for the 2SC/LGB/photon process to start all over again resulting in another emission. For the subsequent emission, however, we expect the system to evolve to point  $\mathbf{B}_1$  generally located at different densities and temperatures than  $\mathbf{B}_0$ . The cycle ends after  $N$  emissions when  $\rho(\mathbf{B}_N) \simeq \rho_{HQS}$ .

The time it takes to consume most of the star (the glue component) by this process is

$$t_{engine} \simeq \frac{M_{HQS} c^2}{L_\gamma} \simeq 1 \text{ s} \left( \frac{M_{HQS}}{M_\odot} \right) \left( \frac{5 \text{ km}}{R_{HQS}} \right)^2 \left( \frac{30 \text{ MeV}}{T_c} \right)^4, \quad (6)$$

which is representative of the engine's activity. The above assumes quick adjustment of the star following each event, but is not necessarily the case for the most massive stars.

### 3.3 Multiple shell emission

The episodic behavior of the star together with the resulting loaded fireball (we call shell) offers a natural mechanism for multiple shell emission if  $T_c < 30$

MeV. Indeed from eq(5) a higher  $T_c$  value would imply extraction of the entire crust in a single emission and no loading of the subsequent fireballs. Clearly,  $T_c < 30$  MeV must be considered if multiple ejections are to occur<sup>2</sup>.

The fraction ( $f$ ) of the crust extracted in a single event is,

$$\Delta M_{crust} = f M_{crust} . \quad (7)$$

The shell is accelerated with the rest of the fireball converting most of the radiation energy into bulk kinetic energy. The corresponding Lorentz factor we estimate to be,

$$\Gamma_{shell} \simeq \frac{\epsilon M_{HQS}}{f M_{crust}} , \quad (8)$$

where we used eq(2) and eq(7).  $\epsilon$  and  $f$  depend on the star's mass and characterize the two emission regimes in our model.

## 4 The two regimes

When the inner crust density is the neutron drip value, one finds a minimum mass star of  $\sim 0.015 M_\odot$ . For masses above this critical value, the corresponding crusts are thin and light. They do not exceed few kilometers in thickness. Matter at the density of such crusts is a Coulomb lattice of iron and nickel all the way from the inner edge to the surface of the star ([24]). For masses below  $0.015 M_\odot$ , the crust can extend up to thousands of kilometers with densities much below the neutron drip. This allows us to identify two distinct emission regimes for a given  $T_c$  ( $< 30$  MeV).

### 4.1 Light stars ( $M_{HQS} < 0.015 M_\odot$ )

These are objects whose average density is  $\sim \rho_{HQS}$  ( $M_{HQS} \simeq \frac{4\pi}{3} R_{HQS}^3 \rho_{HQS}$ ). The 2SC front extends deeper inside the star ( $\delta_{2SC} \sim 1$ ). The star can be represented by a system close to  $\mathbf{A}_0$  in Figures 2. Each of the few emissions (defined by  $\epsilon$ ) is thus capable of consuming a big portion of the star. Furthermore, the entire crust material can be extracted in a few 2SC/LGB/photon cycles ( $\rho_{crust}/\rho_{drip} \ll 1$ ).

Using eq(6), the few emissions lead to

$$t_{tot} \simeq \text{fraction} \times t_{engine}$$

---

<sup>2</sup>Even if  $T_c$  turns out to be greater than 30 MeV, in which case the entire crust will be blown away (eq(5)), one can imagine mechanisms where crust material is replenished. By accretion, for instance, if the HQS is part of a binary. There are also geometrical considerations where asymmetric emission/ejection can occur due to the rapid rotation of Quark Stars; here only a portion of the crust is extracted at a time. This aspect of the model requires better knowledge of the conditions and environments where HQSs are formed.

$$\simeq \text{fraction} \times 0.25 \text{ s} \left( \frac{M_{HQS}}{0.01 M_{\odot}} \right) \left( \frac{1 \text{ km}}{R_{HQS}} \right)^2 \left( \frac{30 \text{ MeV}}{T_c} \right)^4 , \quad (9)$$

where  $t_{tot}$  is representative of the observable time which takes into account the presence of the crust.

## 4.2 Massive stars ( $M_{HQS} \geq 0.015 M_{\odot}$ )

The surface density of a massive star being that of a light star, defines a standard unit in our model. In other words, the mass of the 2SC layer in a massive star case is

$$\Delta M_{2SC,m} \simeq M_{2SC,l} , \quad (10)$$

where “ $m$ ” and “ $l$ ” stand for massive and light, respectively. It implies

$$\frac{\Delta R_{2SC,m}}{R_{2SC,m}} \simeq \frac{1}{3} \left( \frac{R_l}{R_m} \right)^3 \simeq \frac{1}{3} \left( \frac{1 \text{ km}}{5 \text{ km}} \right)^3 \simeq 0.003 . \quad (11)$$

For a typical star of 5 km in radius, we then estimate a 2SC layer of about 15 meters thick (much larger than the photon mean free path thus justifying the local thermal equilibrium hypothesis). Equivalently,

$$\bar{\epsilon} = \frac{M_l}{M_m} \simeq \left( \frac{1 \text{ km}}{5 \text{ km}} \right)^3 \simeq 0.01 , \quad (12)$$

where  $\bar{\epsilon}$  is the average value. This naturally account for many events (or  $N$  fireballs). The average number of fireballs with which an entire star is consumed is thus

$$N \simeq \frac{1}{\bar{\epsilon}} \simeq 100 . \quad (13)$$

Since most of the crust is at densities close to the neutron drip value, eq(5) implies that only a tiny part of the crust surface material (where  $\rho_{crust} \ll \rho_{drip}$ ) can be extracted by each of the fireballs. This allows for a continuous loading of the fireballs.

The total observable time in our simplified approach is thus,

$$t_{tot} \simeq t_{engine} = 1 \text{ s} \left( \frac{M_{HQS}}{M_{\odot}} \right) \left( \frac{5 \text{ km}}{R_{HQS}} \right)^2 \left( \frac{30 \text{ MeV}}{T_c} \right)^4 . \quad (14)$$

We isolated two regimes:

- (i) Light stars  $\Rightarrow$  short emissions.
- (ii) Massive stars  $\Rightarrow$  long emissions.

It appears, according to BATSE (Burst and Transient Source Experiment detector on the COMPTON-GRO satellite), that the bursts can be classified into two distinct categories: short ( $< 2$  s) bursts and long ( $> 2$  s, typically  $\sim 50$  s) bursts. The black body behavior ( $T_c^4$ ) inherent to our model puts stringent constraints on the value of  $T_c$  which best comply with these observations. Using  $T_c \simeq 10$  MeV, from eq(9) and eq(14) we obtain in the star's rest frame

$$t_{tot} \simeq 81 \text{ s} \left( \frac{M_{HQS}}{M_\odot} \right) \left( \frac{5 \text{ km}}{R_{HQS}} \right)^2, \quad (15)$$

for massive stars (suggestive of long GRBs), and

$$t_{tot} \simeq 2 \text{ s} \left( \frac{M_{HQS}}{0.01 M_\odot} \right) \left( \frac{1 \text{ km}}{R_{HQS}} \right)^2, \quad (16)$$

for light stars (suggestive of short GRBs). There is a clear correlation (almost one to one) between the observed burst time and the time at which the source ejected the specific shell (see Figure 3 in [?], for example). Note that  $T_c \simeq 10$  MeV implies that only a portion of the crust is extracted. This is also consistent with our previous assumption ( $T_c < 30$  MeV) and subsequent calculations.

Eq(15) and eq(16) is simply eq(6) rescaled to the appropriate object size. We separated two regimes due to intrinsic differences in the engine and the crust. From the engine point of view, massive stars generate many more emissions when compared to light ones, and no substantial reduction of the engine time is expected because of the omni-presence of the crust. Another important difference is related to the physics of the multiple re-adjustments following each event which is more pronounced for very massive stars. The latter among other factors is related to  $\epsilon$  which can vary from one event to another.

## 5 Features and predictions

### 5.1 GRB energies

The maximum available energy is when the heaviest HQS ( $M_{HQS,max} \simeq 2M_\odot$ ) is entirely consumed. That is,

$$E_{LGB,max} \simeq 4 \times 10^{54} \text{ ergs} . \quad (17)$$

The corresponding GRB energy is

$$E_{GRB,max} \simeq 1.6 \times 10^{54} \text{ ergs} , \quad (18)$$

where we used a fiducial conversion efficiency of 40%.

Since  $M_{HQS,min} < 0.015M_\odot$  we conclude that,

$$E_{LGB,min} < 3 \times 10^{52} \text{ ergs} , \quad (19)$$



implying

$$E_{GRB,min} < 1.2 \times 10^{52} \text{ ergs} . \quad (20)$$

## 5.2 GRB total duration

From eq(15) and eq(16) we have

$$t_{tot} \simeq 81 \text{ s} , \quad (21)$$

for typical massive stars, and

$$t_{tot} \simeq 2 \text{ s} , \quad (22)$$

for typical light stars.

Our estimate of the duration time for the massive star case should be taken as a lower limit. As we have said, a complete model should take into account star re-adjustments. Nevertheless, we can still account for a wide range in GRB duration by an appropriate choice of different values of the mass and radius.

# 6 Discussion and Conclusion

## 6.1 Existence and formation of HQSs

In the last few years, thanks to the large amount of fresh observational data collected by the new generation of X-ray and  $\gamma$ -ray satellites, new observations suggest that the compact objects associated with the X-ray pulsars, the X-ray bursters, particularly the SAX J1808.4-3658, are good quark stars candidates (see Bombaci in this volume and [29]). If one assumes that these plausible quark stars form via the “standard” supernova mechanism or by conversion of neutron stars then the two regimes (Heavy and Light stars) discussed in our model are difficult to account for. It has been argued however that quark stars formation mechanisms may be numerous and “exotic” (early discussions can be found in [30, 23]). In the case of 4U 1728-34 (where a mass of less than  $1.0M_{\odot}$  was derived; [14]), it seems that accretion-induced collapse of white dwarfs is a favored formation mechanism. If the quark star formed via the direct conversion mechanism then it required too much mass (at least  $\sim 0.8M_{\odot}$  to be ejected during the conversion). Other formation scenarios are discussed in [31, 32].

## 6.2 Neutrino cooling and HQSs

If it turns out that neutrino cooling is still very efficient in the 2SC phase, one must consider the scenario where the entire HQS enters the 2SC phase (for comparison of cooling paths between quark stars and neutron stars and the

plausible effects of 2SC on cooling we refer the interested reader to [26, 33, 34]. Here, the 2SC/LGB/photon process (the fireball) occurs only once and inside the entire star. Furthermore, one must involve more complicated physics (such as that of the crust) to account for the episodic emissions so crucial to any model of GRBs. It is not clear at the moment how to achieve this goal and is left as an avenue for future research.

### 6.3 2SC-II stars

The 2SC/LGB/photon process might proceed until one is left with an object made entirely of 2SC. We name such objects *2SC-II* stars<sup>3</sup> which are still bound by strong interactions (their density is constant  $\sim \rho_{HQS}$ ). 2SC-II stars carry an Iron/Nickel crust left over from the GRB phase. The crust mass range is  $0 < M_{2SC,crust} < 5 \times 10^{-5} M_{\odot}$  depending on the efficiency of crust extraction/ejection during the GRB phase.

BATSE observes on average one burst per day. This corresponds, with the simplest model - assuming no cosmic evolution of the rate - to about once per million years in a galaxy [3]. In the Milky way we thus expect up to  $10^5$  of 2SC-II stars. Nevertheless, they are tiny enough ( $M \leq 10^{-2} M_{\odot}$ ,  $R \leq 1$  km) to be difficult to detect.

### 6.4 The Mass–Radius Plane

Take observed GRBs with known energies and total duration. From the burst total energy  $E_{GRB} \simeq 0.4 M c^2$  we derive the mass while the burst total duration ( $t_{tot}$ ) gives us the radius (using eq(14) with  $T_c \simeq 10$  MeV). In Figure 3 we plot the resulting Mass–Radius. The solid curve shows the  $M_{HQS} = \frac{4\pi}{3} \rho_{HQS} R_{HQS}^3$  equation which is a reasonable approximation for HQSs. While the GRB data set used is limited nevertheless it seems to support the idea that extremely compact objects ( $M \propto R^3$ ) are behind GRBs activity within our model.

## References

- [1] Kouveliotou, C., Briggs, M. S., and Fishman, G. J., (Eds), Gamma Ray Bursts, AIP Conf. Proc., 384 (AIP, New York, 1995)
- [2] Kulkarni, S. R., et al., Nature, **398**, 389 (1999)
- [3] Piran, T., Phys. Rev., **314**, 575 (1999a)
- [4] Piran, T., in Gamma-Ray Bursts: The first three minutes, ASP Conference Series, Vol. 190, eds. J. Poutanen and R. Svensson, 3 (1999b)

---

<sup>3</sup>The “II” in 2SC is a simple reminder of the final state of the star, namely the 2SC with only 5 gluons.

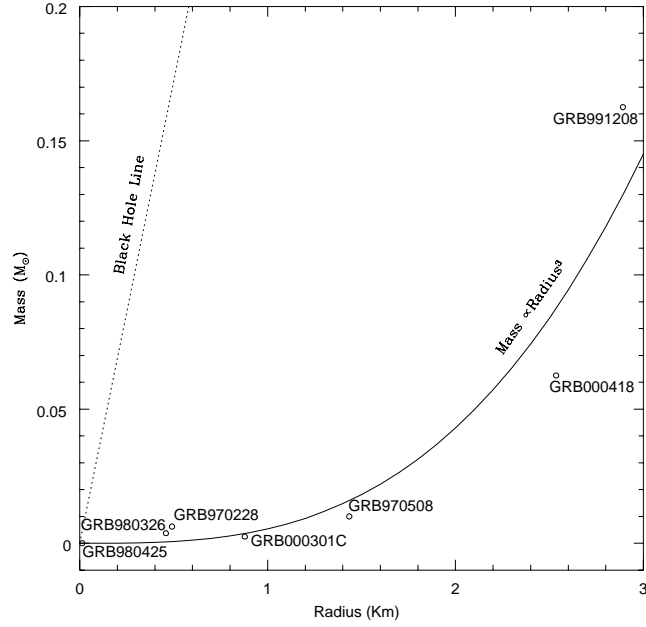


Figure 3: The Mass–Radius plane derived in our model using few existing GRBs with known energies and total duration. The solid curve shows the  $M_{HQS} = \frac{4\pi}{3}\rho_{HQS}R_{HQS}^3$  equation for  $\rho_{HQS} \simeq 9\rho_N$ .

- [5] Goodman, J., ApJ, **308**, L47 (1986)
- [6] Shemi, A., and Piran, T., ApJ, **365**, L55 (1990)
- [7] Paczyński, B., ApJ, **363**, 218 (1990)
- [8] Ouyed, R., and Sannino, F., Phys. Lett. **B511**, 66 (2001a)
- [9] Blandford, R. D., and Znajek, R. L., MNRAS, **179**, 433 (1977)
- [10] Ruffert, M., and Janka, H. -T., A&A, **344**, 573 (1999)
- [11] Janka, H. -T., Eberl, T., Ruffert, M., and Fryer, C., ApJ, **527**, L39 (1999)
- [12] Olinto, A., Phys. Lett. **B192**, 71 (1987)
- [13] Cheng, K. S., and Dai, Z. G., Phys. Rev. Lett., **77**, 1210 (1996)
- [14] Bombaci, I, and Datta, B., ApJ, **530**, L69 (2000)
- [15] Ouyed, R., and Sannino, F., astro-ph/0103022 (2001b)
- [16] Bodmer, A. R., Phys. Rev. **D4**, 1601 (1971)
- [17] Witten, E., Phys. Rev. **D30**, 272 (1984)
- [18] Haensel, P., Zdunik, J. L., and Schaefer, R., A&A, **160**, 121 (1986)

- [19] Alcock, C., Farhi, E., and Olinto, A., *ApJ*, **310**, 261 (1986)
- [20] Dey, M., Bombaci, I., Dey, J., Ray, S., and Samanta, B. C., *Phys. Lett.* **B438**, 123 (1998)
- [21] Farhi, E., and Jaffe, R. L., *Phys. Rev.* **D30**, 2379 (1984)
- [22] Glendenning, N. K., and Weber, F., *ApJ*, **400**, 647 (1992)
- [23] Glendenning, N. K., *Compact stars* (Springer, 1997)
- [24] Baym, G., Pethick, C. J., and Sutherland, P. G., *ApJ*, **170**, 299 (1971)
- [25] Carter, G. W., and Reddy, S., [hep-ph/0005228](#)
- [26] Schaab, C., Hermann, B., Weber, F., and Manfred, K., *ApJ*, **480**, L111 (2000)
- [27] Rybicki, G. B., and Lightman, A. P. *Radiative processes in astrophysics* (Wiley, 1979)
- [28] Longair, M. S., *High energy astrophysics* (Cambridge Univ. Press, 1992)
- [29] Li, et al., *Phys. Rev. Lett.*, **83**, 3776 (1999)
- [30] Alpar, A. M., *Phys. Rev. Lett.*, **58**, 2152 (1987)
- [31] Hong, D. K., Hsu, S. D. H., and Sannino, F., *Phys. Lett. B*, in press ([hep-ph/0107017](#))
- [32] Ouyed, R., Dey, J., and Dey, M., [astro-ph/0105109](#)
- [33] Blaschke, D., Klähn, T., and Voskresensky, D. N., *ApJ*, **533**, 406 (2000)
- [34] Blaschke, D., Grigorian, H., and Voskresensky, D. N., *A&A*, **368**, 561 (2001)